

SIMULATION OF LAND MOBILE SATCOM LINKS USING DIFFERENT ORBITS AND MODULATION MODES

Marcel Kohl and Friedrich Jondral
Universität Karlsruhe, Nachrichtensysteme
D-76128 Karlsruhe, Germany
Tel: +49 721 6083748; fax: +49 721 6086071
e-mail: kohl@inss1.etec.uni-karlsruhe.de

ABSTRACT

The use of SATCOM systems is an essential part of today's worldwide communications. As the portion of satellite orbits in low altitudes increases, Doppler shifts often influence the received signal. Prior to the removal of this effect, the exact course and the amount of the Doppler must be known. Therefore this paper derives the equations to calculate the orbit and the Doppler shift and shows the behaviour and the effects caused by LEO and HEO satellites. Finally a method is proposed to compensate this influence.

1 INTRODUCTION

Transmission of multimedia services is done on information highways, which are supported by optical fiber links. The data rates of the information highways are in the range of 1 to 2 Gbit/s, and there are test installations with data rates of 10 Gbit/s [1]. The large business centers are already connected by a optical fiber networks. The connection of the remaining areas can only be achieved with satellite communication networks, and such a network should provide sufficient transmission capacities.

In satellite communication (SATCOM) systems especially the high bandwidth requirements can only be met in the higher frequency ranges, i.e. in the K-band (18–26.5 GHz) and above. Until now many investigations in these ranges have been carried out from a physical point of view. But the overall system aspects have not been investigated, i.e. how to choose system characteristics for example transmitter power, preferable orbits, modulation mode, coding, etc. The present paper shows an analysis of the expected Doppler shifts of a land mobile SATCOM link in the K-band.

2 MODEL

The simulation model considers all elements of a satellite transmission link, i.e. transmitter, uplink and receiver. These elements are explained below.

2.1 Transmitter

This element provides the simulation with a modulated signal. It consists of a binary source (pseudo-noise sequence) which feeds a synchronization frame, a modulator with impulse shaping (square root raised cosine roll-off) [2] and an amplifier. The synchronization frame is used within the coherent demodulator in the receiver for carrier synchronization. The sampling rate is increased during the impulse shaping by a factor between 4 and 16 to simulate a sufficiently large channel bandwidth.

2.2 Receiver

The receiver is modelled by a preamplifier and a pre-selection filter followed by a controllable amplifier and a main selection filter corresponding to the square root raised cosine roll-off filter used in the transmitter. Synchronous demodulation needs both clock [3] and carrier recovery [4]. Therefore they precede the coherent demodulator, which uses the synchronization frame. At the output the bit error rate (BER) is determined.

2.3 Channel

Here the name channel refers to the whole path between the output of the transmitter and the input of the receiver, i.e. the antennas also belong to the channel.

The influences of the antennas are determined by their geometry and alignment with each other. The effect of antenna geometry on the radiation is described by the frequency dependent antenna diagram [5]. Additionally, noise components due to thermal noise must be considered at the receiving antenna [5, 6]. The noise of electronic components, i.e. amplifiers, is taken into account by additive white Gaussian noise sources at the subsystem's inputs.

The atmosphere is essentially divided into two regions: The troposphere and the ionosphere. Attenuations, depolarizations and scintillations [7, 8] modify each signal, which passes through the two regions. The physical effect of the electromagnetic influences may be transformed into attenuations at the receiver. Therefore all effects are modelled by attenuations.

The free space loss is calculated by

$$L_{FS} = \left(\frac{4\pi r f}{c} \right)^2 \quad (1)$$

expressing the ratio of the radiated to the received power between two isotropic antennas with distance r at the frequency f . c is the velocity of light.

The transponder connects up- and downlink. It is composed of a low noise amplifier and a transponder filter, which reduces spectral components outside the transponder band, e.g. noise. A travelling wave tube (TWT) is used as power amplifier followed by a second filter reducing the out of band intermodulations.

3 DOPPLER SHIFT

Doppler shifts exist due to the movement of a transmitter or a receiver relative to its counterpart. A frequency shift of

$$\Delta f_D = f_c \frac{v}{c} \quad (2)$$

results, where f_c is the carrier frequency and v is the relative velocity. Two reasons cause Doppler shifts of a SATCOM link: Movements of mobile users on earth and satellites in non geosynchronous orbits (non-GEO). Doppler shifts of mobile users are modelled by Doppler spectra as described in [9]. These may be used for land mobile SATCOM links too, assuming uniformly distributed arrival angles of the reflected paths.

Accepting that

- the satellite mass m_S may be neglected in comparison to the earth's mass M_E ,
- the earth is spherical and homogeneous and
- the two body system earth-satellite is isolated (e.g. there are no disturbing influences caused by the sun, the moon, or by other celestial bodies),

the satellite's location vector \vec{r} is described by a vector differential equation of second order [10], resulting from the identification of the gravity

$$\vec{F}_s = - \frac{GM_E m_S}{|\vec{r}|^2} \frac{\vec{r}}{|\vec{r}|} \quad (3)$$

affecting the satellite and the centrifugal force

$$\vec{F}_Z = m_S \frac{d^2 \vec{r}}{dt^2} \quad (4)$$

originating from the satellite's movement. The product $G \cdot M_E$ of the universal gravitation constant G and the earth's mass is the Keplerian constant $\mu = 3.9861352 \cdot 10^5 \text{ km}^3/\text{s}^2$.

Using the differential equation resulting from eq. (3) and eq. (4) it can be shown that the angular momentum vector

$$\vec{h} = \vec{r} \times \frac{d\vec{r}}{dt} \quad (5)$$

is constant. From this it is concluded, that the satellite's orbit lies in a (two dimensional) plane. The solution of the differential equation is computed in a coordinate system, the x-y-plane of which coincides with the orbital plane. Written in polar coordinates (r_0, ϕ_0) with the semilatus rectum p and the eccentricity e , the solution is

$$r_0 = \frac{p}{1 + e \cos(\phi_0 - \theta_0)}, \quad 0 \leq e < 1, \quad (6)$$

i.e. the orbit of a communications satellite is an ellipse with orientation θ_0 .

To get a unique solution of the three dimensional vector differential equation for the satellite's location vector \vec{r} , six orbital parameters must be predetermined. The usual parameter set is [10]:

1. The ellipse's eccentricity,
2. its semimajor axis,
3. the time of perigee,
4. the right ascension of the ascending node,
5. the orbit's inclination and
6. the argument of perigee.

For ease of calculation the origin of the geocentric coordinate system is shifted to the location of the mobile user terminal. The Doppler is computed by eq. (2) using the time derivative of the satellite's location. A closed form solution is available only for circular orbits [11]. All other cases must be treated numerically. A general approach is discussed in [12].

Some Doppler profiles of a low earth orbit (LEO) and a highly inclined elliptical orbit (HEO) are shown in Fig. 1–3 as examples. The calculation of the profiles starts with an earth station situated on the ground track of the satellite (projection of the orbit onto the earth's surface). Each position along the ground track represents the subsatellite point for a certain time. Then the earth station is moved to the east and to the west at a fixed latitude until the orbit is out of view, i.e. the elevation is less than zero. The Doppler shift is calculated at a carrier frequency of 18 GHz for each of these positions over time. The figures are parametrized with the deviation of the earth station's position in degrees longitude from the ground track. The Doppler shift is set to zero if the elevation is less than zero.

In Fig. 1 only earth stations moved to the west are shown due to no differences regarding earth stations to the east. The visibility of the satellite at 0° is approximately 700 s. The Doppler varies considerably and is influenced by the earth's rotation. Therefore the curves are not symmetric to their intersection with the time axis. Fig. 2 shows the results for an orbit with 135° inclination. In comparison to Fig. 1 the Doppler shift is increased through the strengthened influence of the earth's rotation. Fig. 3 illustrates the Doppler of a polar HEO satellite below the apogee. At the beginning of

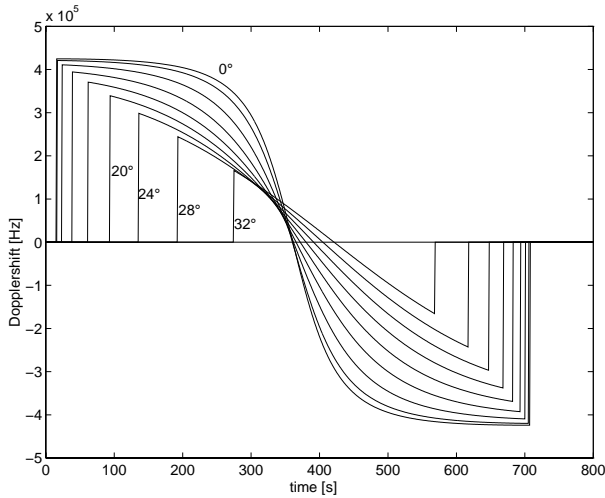


Fig. 1: Polar circular orbit, 90° inclination, orbit altitude 500 km, earth station at 50° latitude.

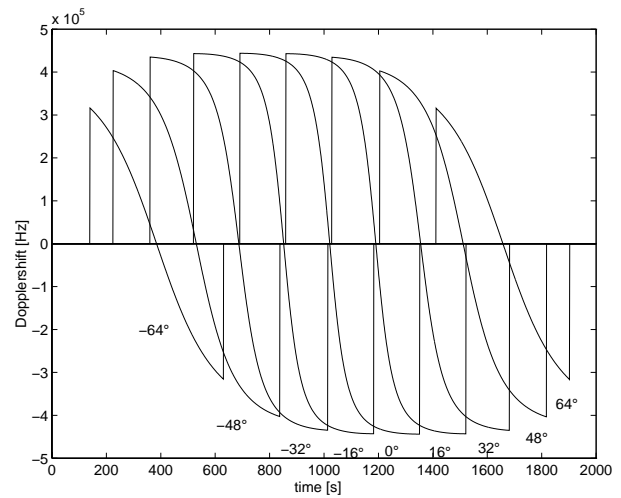


Fig. 2: Circular orbit, 135° inclination, orbit altitude 500 km, earth station at 45° latitude.

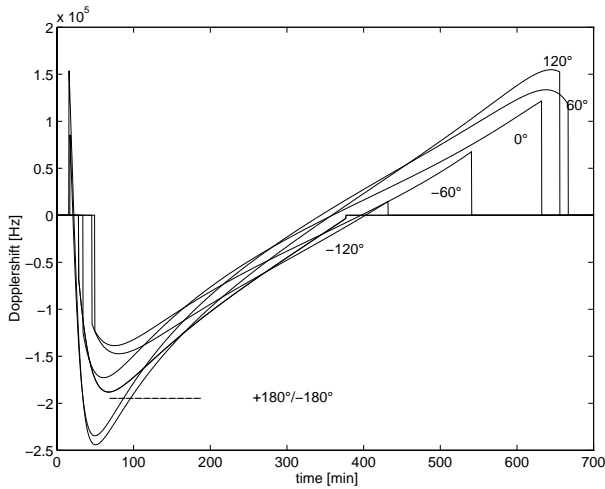


Fig. 3: Polar HEO, 90° inclination, earth station at 50° latitude below apogee (39362 km).

the visibility range the Doppler rate is negative because the satellite distance increases to approach the apogee. Then the Doppler shift reaches its maximum and turns into a slight positive Doppler rate. This is the main region for link establishment and transmission due to the high elevation angle. Note, that in comparison to the other examples the time scale has changed and the visibility has grown to about 11 hours. In Table 1 the main points of the examples are summarized.

4 RESULTS

For LEO satellites the Doppler profiles show very high absolute Doppler shifts and a dramatic Doppler rate (Table 1) in the middle of the observation interval. Therefore a good carrier control loop is needed for a reliable transmission. Such a carrier control loop should have the following properties: Adaptation to the fast varying Doppler shifts and synchronization to signals

| | max. shift | max. rate |
|--------|------------|-----------|
| Fig. 1 | 425 | 6475 |
| Fig. 2 | 444 | 7282 |
| Fig. 3 | 191 | 0.08* |

* main region

Table 1: Doppler shift and Doppler rate in kHz.

outside the user bandwidth, due to the high Doppler shift, which in general is the case at the beginning of the satellite's observation interval. But because of the lack of a signal the latter is not achievable. This starting frequency offset must be known before by the control loop approximately. This means each terminal has to calculate the Doppler shift from the orbit parameters at the time of connection set-up. Signals with large bandwidths, e.g. multimedia services or spread spectrum signals, might overcome this problem since the maximal Doppler offset is small compared to the user bandwidth.

The normal control operation is performed by various control loops depending on the modulation mode. In [13] a technique for estimating and correcting Doppler shifts is shown using multiple differential phase shift-keying (MDPSK). Another approach is described in [14] for a double differential phase shift

keying (DDPSK) receiver.

All these methods need an accompanying calculation of the Doppler shift to improve the BER near to its maximum. Due to the need of a Doppler calculation at the beginning this may also be useful during the whole transmission. The known Doppler corrects the oscillator frequency of the receiver at any time instant. In the receiver the signal is always downconverted into the baseband. The task of a carrier control loop is reduced to minor corrections of the frequency. This can be performed by an ordinary phase locked loop (PLL) as described in [15].

5 SUMMARY

In particular for the Doppler shift, we have presented a tool for its calculation. The Doppler profiles shown, give an impression of the difficulties regarding the reception of such disturbed signals. Especially receivers of LEO SATCOM systems demand for a good and fast carrier control loop. But due to the high amount of frequency offsets it is necessary to calculate in advance the Doppler shift. Additionally this may be used to compensate the Doppler at the receiver and to reduce the complexity of its carrier control loops.

6 REFERENCES

- [1] C. Josenhans. Digitales HDTV-Interface. Bericht im Rahmen des Forschungsverbundes Medientechnik Südwest, Nachrichtensysteme, Universität Karlsruhe, 1995.
- [2] J.G. Proakis and S. Masoud. *Communication Systems Engineering*. Prentice-Hall, Inc., Englewood Cliffs, NJ, 1994.
- [3] F.M. Gardner. Interpolation in digital modems - part I: Fundamentals. *IEEE Trans. on COM*, 41(3):501–507, March 1993.
- [4] M.C. Jeruchim, P. Balaban, and K.S. Shanmugan. *Simulation of Communication Systems*. Plenum Press, New York, 1994.
- [5] G. Maral and M. Bousquet. *Satellite Communications Systems*. Teubner, 2nd edition, 1993.
- [6] E.G. Njoku and E.K. Smith. Microwave antenna temperature of the earth from geostationary orbit. *Radio Science*, 20(3):591–599, May/June 1985.
- [7] D.C. Cox and H.W. Arnold. Results from the 19- and 28-GHz COMSTAR satellite propagation experiments at Crawford Hill. *Proc. of the IEEE*, 70(5):458–488, May 1982.
- [8] R. Jakoby and F. Rucker. Three years of crosspolar measurements at 12.5, 20 and 30 GHz with the OLYMPUS satellite. In *OLYMPUS utilisation Conference*, pages 567–572, Seville, Spain, April 1993.
- [9] W.C. Jakes Jr. *Microwave Mobile Communications*, chapter 1, pages 11–78. John Wiley & Sons, Inc., 1974.
- [10] T. Pratt and C.W. Bostian. *Satellite Communications*. John Wiley & Sons, New York, 1986.
- [11] M.J. Miller, B. Vucetic, and L. Berry. *Satellite Communications: Mobile and Fixed Services*. Kluwer Academic Publishers, Dordrecht (The Netherlands), 1993.
- [12] F. Jondral, M. Kohl, and C. Hartmann. Doppler-profile für Kommunikationssatelliten. *Frequenz*, 50(5-6), 1996.
- [13] M.K. Simon and D. Divsalar. Doppler-corrected differential detection of MPSK. *IEEE Trans. on COM*, 37(2):99–109, February 1989.
- [14] M.K. Simon and D. Divsalar. On the implementation and performance of single and double differential detection schemes. *IEEE Trans. on COM*, 40(2):278–291, February 1992.
- [15] H. Meyr and G. Ascheid. *Synchronisation in Digital Communications*, volume 1. John Wiley & Sons, 1990.